Dissipative shape dynamics in the *sd* shell

M. Grigorescu and N. Carjan*
Department of Theoretical Physics, Institute of Atomic Physics, P.O. Box MG 6, Bucharest, R-76900, Romania
(Received 14 March 1996)

The coupling between the nuclear shape dynamics and the internal degrees of freedom is investigated in the frame of a time-dependent Hartree-Fock-Bogolyubov Langevin formalism. The shape coordinate considered here is the quadrupole deformation, and the internal configuration space is restricted to the *sd* shell. The numerical results concern the effects of pairing, dissipation, and temperature on the giant quadrupole shape vibration of ^{28}Si. Time scales for decay, thermalization, and configuration transitions are obtained. [S0556-2813(96)05108-4]

PACS number(s): 21.60.Jz, 21.60.Ev, 24.10.Cn, 24.30.Cz

I. INTRODUCTION

The change in the internal structure of the nucleus during large amplitude collective motion is the basic process for particle emission or fission-fusion reactions. At low excitation energies the mean free path of the nucleons is large, and they interact basically only with the time-dependent mean field [1]. In this case, the simple classical model of an elastic container filled with gas at very low pressure shows the occurrence of one-body dissipation [2]. This mechanism was used especially in the study of the fission process [3,4], reproducing well the neutron multiplicities and the kinetic energies of the fragments [5].

In this approach a first limitation is introduced by the treatment of the time-dependent mean field, which is not self-consistent, but acts like an external force. For instance, the internal motion is regular during forced quadrupole shape oscillations, but it becomes chaotic in a self-consistent calculation [6]. In addition, the assumption of the complete disappearance of two-particle pairing correlations may be not realistic. At low excitation energy the nucleus ressembles a superfluid Fermi droplet, and the irreversible changes of the nuclear shape are strongly connected to the superfluidity [7].

The purpose of this paper is to investigate the effects of pairing and temperature on the nuclear quadrupole shape dynamics. Systems in thermal equilibrium at high excitation energy were studied using coupled variational equations for the static Hartree-Fock mean field and entropy [8]. In the present work, the system is not supposed to be equilibrated, and the time-dependent Hartree-Fock-Bogolyubov (TDHFB) mean-field equations are coupled to a classical thermal environment, represented by a bath of harmonic oscillators. Therefore, evolution towards thermalization can be studied dynamically, solving a set of generalized TDHFB-Langevin equations. These equations are derived in Sec. II following the variational procedure applied before to the time-dependent Schrödinger equation [9]. Compared to the calculations based on transport equations, this approach has the quality of including the quantum effects at the same level as the TDHFB approach does. Therefore, it seems to be the best suited for the study of the combined effect produced by pairing and temperature in large amplitude collective motion.

For applications to the giant quadrupole resonance (GQR) the general TDHFB-Langevin equations are constrained to account for only the quadrupole shape deformation and occupation number degrees of freedom. The restriction should preserve the original Hamiltonian structure of the TDHFB equations and is not trivial. The trial manifolds and the basic dynamical equations for a single oscillator shell are presented in Sec. III.

The environment is supposed to represent the intrinsic and collective deegrees of freedom which are fast relatively to the quadrupole vibration [10], and also which are responsible for its decay. The increase of the decay width for decreasing nuclear volume (mass) is similar to the behavior of damping in viscous systems, and was accounted for by hydrodynamic models with two-body dissipation [11]. Beside this general trend, the GQR widths are particularly small near closed shell nuclei [12]. This fact indicates that the GQR dynamics depends also on details of nuclear structure which can be accounted for properly only in microscopic models. The TDHFB-Langevin approach includes the shell effects, and can be applied to study the GQR dynamics. Numerical results obtained for ^{28}Si are presented in Sec. IV. Conclusions are summarized in Sec. V.

II. TDHFB-LANGEVIN EQUATIONS

Let us denote by $\mathbf{H}_0$ the microscopic nuclear Hamiltonian, and by $\mathcal{S}=\{|\Psi\rangle(X)\}$ the trial manifold of normed HFB functions within a model space containing N_s states. The coordinates on $\mathcal{S}$, denoted $X=\{x^i\}$, $i=1,2N, N=N_s(N_s-1)/2$, can be chosen to be the parameters of the general Bogoliubov transformation [13], and $\omega^{\mathcal{S}}$ is the matrix $\omega^{\mathcal{S}}=[\omega^{\mathcal{S}}_{ij}(\Psi)]$, defined by

$$\omega^{\mathcal{S}}_{ij}(\Psi)=2\hbar\,\mathrm{Im}\langle\partial_i\Psi|\partial_j\Psi\rangle. \tag{1}$$

*Permanent address: Centre d'Etudes Nucléaires de Bordeaux-Gradignan, IN2P3-CNRS/Université Bordeaux I, BP 120, F-33175, Gradignan Cedex, France.

In this case, the TDHFB equations can be derived from the stationarity condition of the functional $\mathcal{J}[X] = \int \langle \Psi | i\hbar \partial_t - \mathbf{H}_0 | \Psi \rangle dt$ with respect to small variations of the trajectories X_t, and can be expressed in the form of the Hamilton system of equations [14]

$$\sum_{j=1}^{2N} \dot{x}^j \omega_{jk}^{\mathcal{S}}(\Psi) = \frac{\partial \langle \Psi | \mathbf{H}_0 | \Psi \rangle}{\partial x^k}. \tag{2}$$

Therefore, the variational equation $\delta_\psi \mathcal{J}[X] = 0$ has the solution $|\Psi\rangle(X_t)$, with X_t a trajectory given by Eq. (2).

Let us consider now a many-body system which is coupled bilinearly to a bath of N_c classical harmonic oscillators. Within the same mean field approximation, the evolution can be obtained using the variational equation

$$\delta_{\Psi, q_i} \int dt \sum_{i=1}^{N_c} m_i (\dot{q}_i)^2 + \langle \Psi | i\hbar \partial_t - \mathbf{H} | \Psi \rangle = 0, \tag{3}$$

where $\mathbf{H} = \mathbf{H}_0 + \mathbf{H}_b$, $\mathbf{H}_0$ is the Hamiltonian operator without bath coupling, and

$$\mathbf{H}_b = \sum_{i=1}^{N_c} \left[\frac{m_i \dot{q}_i^{\,2}}{2} + \frac{m_i \omega_i^2}{2} \left(q_i + \frac{C_i}{m_i \omega_i^2} \mathbf{K} \right)^2 \right] \tag{4}$$

represents the bath energy plus the coupling interaction. Performing the variations with respect to $X(t)$ and the bath trajectories $q_i(t)$, the coupled equations of motion are

$$\begin{aligned} \sum_{j=1}^{2N} \dot{x}^j \omega_{jk}^{\mathcal{S}}(\Psi) = {} & \frac{\partial \langle \Psi | \mathbf{H}_0 | \Psi \rangle}{\partial x^k} \\ & + \frac{\partial \langle \Psi | \mathbf{K}^2 | \Psi \rangle}{\partial x^k} \sum_{i=1}^{N_c} \frac{C_i g_i}{2} \\ & + \frac{\partial \langle \Psi | \mathbf{K} | \Psi \rangle}{\partial x^k} \sum_{i=1}^{N_c} C_i q_i, \end{aligned} \tag{5}$$

with $g_i = C_i / m_i \omega_i^2$ and

$$\begin{aligned} \dot{q}_i &= \frac{p_i}{m_i}, \\ \dot{p}_i &= -m_i \omega_i^2 q_i - C_i \langle \Psi | \mathbf{K} | \Psi \rangle. \end{aligned} \tag{6}$$

Equations (6) may be solved in terms of the unknown function of time $\langle \Psi | \mathbf{K} | \Psi \rangle$, and when their retarded solution is inserted in Eq. (5) we obtain a Langevin form of Eq. (2) [15],

$$\begin{aligned} \sum_{j=1}^{2N} \dot{x}^j \omega_{jk}^{\mathcal{S}}(\Psi) = {} & \frac{\partial \langle \Psi | \mathbf{H}_0 + \mathbf{W}_{\rm ren} | \Psi \rangle}{\partial x^k} - \frac{\partial \langle \Psi | \mathbf{K} | \Psi \rangle}{\partial x^k} \\ & \times \left[\xi(t) - \int_0^t \Gamma(t - t') \frac{\partial \langle \Psi | \mathbf{K} | \Psi \rangle}{dt'} dt' \right]. \end{aligned} \tag{7}$$

Here

$$\mathbf{W}_{\rm ren} = (\mathbf{K}^2 - \langle \Psi | \mathbf{K} | \Psi \rangle \mathbf{K}) \frac{\Gamma(0)}{2}$$

and

$$\Gamma(t) = \sum_{i=1}^{N_c} g_i C_i \cos \omega_i t \equiv \frac{2}{\pi} \int_0^\infty d\omega J(\omega) \frac{\cos \omega t}{\omega}.$$

$\mathbf{W}_{\rm ren}$ can be considered as a renormalization of the interaction term in $\mathbf{H}$, and it will be neglected. $\xi(t)$ represents the noise, and is related to $\Gamma(t)$ (the ''memory function'') by the fluctuation-dissipation theorem $\langle\langle \xi(t) \xi(s) \rangle\rangle = k_B T \Gamma(t - s)$, the double brackets meaning statistical averaging over the bath ensemble [16].

The spectral density of the bath, $J(\omega)$, for white-noise (linear friction) and blackbody radiation is presented in [17], discussing the possible transition from a radiation reaction to an elastic response (elastoplastic behavior). For linear friction, $\Gamma(t) = 2 \gamma_K \delta(t)$, with γ_K the static friction coefficient. In this case Eq. (7) takes the form

$$\begin{aligned} \sum_{j=1}^{2N} \dot{x}^j \omega_{jk}^{\mathcal{S}}(\Psi) = {} & \frac{\partial \langle \Psi | \mathbf{H}_0 | \Psi \rangle}{\partial x^k} - \frac{\partial \langle \Psi | \mathbf{K} | \Psi \rangle}{\partial x^k} \\ & \times \left[\xi(t) - \gamma_K \frac{d \langle \Psi | \mathbf{K} | \Psi \rangle}{dt} \right]. \end{aligned} \tag{8}$$

At $T = 0$ the noise vanishes, and the energy $E = \langle \Psi | \mathbf{H}_0 | \Psi \rangle$ is dissipated according to the law

$$\frac{dE}{dt} = -\gamma_K \left(\frac{d \langle \mathbf{K} \rangle}{dt} \right)^2. \tag{9}$$

The system may reach in this case the HFB ground state (g.s.) with energy $E_{\rm g.s.}$.

When $T > 0$, the asymptotic value of the excitation energy $E_x(t) = E(t) - E_{\rm g.s.}$ fluctuates around an average E_f depending on the number of thermalized degrees of freedom which contribute to the specific heat of the system. If the quadrupole vibrations are the only possible motion, then $E_f = k_B T$, and represents the average energy of the shape fluctuations.

The friction constant γ_K is given by the spectral density of the environment. Therefore, it can be calculated if the parameters of the bath oscillators as well as the strength of coupling are known.

III. RESTRICTED TDHFB-LANGEVIN APPROACH FOR QUADRUPOLE AND PAIRING DYNAMICS

The HFB trial functions have a complicated structure, accounting for many degrees of freedom of the nucleus. Therefore, to study only quadrupole and pairing dynamics, the trial functions will be restricted to submanifolds of $\mathcal{S}$, parametrized by the phase space coordinates for the quadrupole motion and the pairing variables.

The quadrupole deformation parameter β_2 appears both in collective and microscopic models of the nucleus [18]. Phenomenologically, it is a mean-field parameter which can be extracted from the measured $B(E2)$ transition rate between the 0^+ ground state and the first 2^+ excited state [19].

The g.s. axial deformation breaks the rotational symmetry and appears spontaneously, to lower the level density of the spherical mean field. Microscopically, this means a change in the single-particle (s.p.) basis which is used to construct

the g.s. many-body wave function, and a rearrangement of the A nucleons on the new orbitals. The observable related to this change is the g.s. expected value $\langle \mathbf{Q}_0 \rangle$ of the $\mu=0$ component of the quadrupole operator, $\mathbf{Q}_0 = \Sigma_{i=1,A} \sqrt{5/16\pi}(2z^2-x^2-y^2)_i$.

For excited configurations, $\langle \mathbf{Q}_0 \rangle$ depends on time, such that

$$\frac{d\langle \Psi|\mathbf{Q}_0|\Psi\rangle}{dt} = \frac{i}{\hbar}\langle \Psi|[\mathbf{H}_0,\mathbf{Q}_0]|\Psi\rangle \tag{10}$$

(the Ehrenfest theorem). Therefore, to study the shape dynamics, a minimal requirement is to construct many-body trial states $|\Psi\rangle$ where the single-particle basis depends continuously on the deformation coordinate and velocity, and allowing for the change of the occupation probabilities.

Following the procedure applied before to spontaneously symmetry breaking systems [20], if $[\mathbf{H}_0,\mathbf{Q}_0]\neq 0$, then a two-parameter family of ''yrast'' states $|\Psi\rangle$ can be constructed having a classical phase-space structure, and the lowest energy compatible with fixed expected values for the quadrupole momentum $\langle \mathbf{Q}_0 \rangle$ and velocity, $d\langle \mathbf{Q}_0 \rangle/dt$. Such many-body wave functions are the extrema of the cranking variational equation

$$\delta_\Psi \langle \Psi|\mathbf{H}_0 - \lambda_q \mathbf{Q}_0 - \lambda_v \frac{i}{\hbar}[\mathbf{H}_0,\mathbf{Q}_0]|\Psi\rangle = 0 \tag{11}$$

and are parametrized by the Lagrange multipliers λ_q, λ_v. However, when Eq. (11) is solved and the functions $|\Psi(\lambda_q,\lambda_v)\rangle$ are known, the parametrization can be changed, if desired, using $\langle \mathbf{Q}_0 \rangle$ and $d\langle \mathbf{Q}_0 \rangle/dt$ as new variables.

The ''velocity'' operator may be easily calculated in the harmonic oscillator approximation. This approximation was proved to be relevant for the microscopic description of the fusion/fission reactions of light nuclei [21], being successfully used in the Harvey model [22]. Let us denote by $\mathbf{h}_0$ the s.p. isotropic oscillator Hamiltonian

$$\mathbf{h}_0 = \sum_{j=x,y,z} \hbar\omega_0(\mathbf{b}_j^\dagger \mathbf{b}_j + 1/2),$$

with $\mathbf{b}_j^\dagger = \sqrt{m\omega_0/2\hbar}(x_j - ip_j/m\omega_0)$, $\omega_0 = 41A^{-1/3}$ MeV/$\hbar$, and by $\mathbf{K}$ the dimensionless quadrupole operator $\mathbf{K}=\mathbf{Q}_0/c_0$, with $c_0=(5/4\pi)^{1/2}\hbar/m\omega_0 = 26.17$ MeV fm^2/$\hbar\omega_0$,

$$\mathbf{K} = 2\mathbf{K}_z - \mathbf{K}_x - \mathbf{K}_y, \quad \mathbf{K}_j = \sum_{i=1,A} (\mathbf{k}_j)_i. \tag{12}$$

Here $\mathbf{k}_j = m\omega_0 \mathbf{x}_j^2/2\hbar = \mathbf{s}_{1,j} + \mathbf{s}_{3,j}$, with

$$\mathbf{s}_{1,j} = [(\mathbf{b}^\dagger)_j^2 + \mathbf{b}_j^2]/4, \quad \mathbf{s}_{3,j} = (\mathbf{b}_j^\dagger \mathbf{b}_j + 1/2)/2. \tag{13}$$

If $\mathbf{H}_0$ is reduced to the spherical harmonic oscillator term,

$$\mathbf{H}_0 = \sum_{i=1,A} (\mathbf{h}_0)_i = 2\hbar\omega_0 \sum_{i=1,A} (\mathbf{s}_{3,x} + \mathbf{s}_{3,y} + \mathbf{s}_{3,z})_i,$$

the velocity operator is given up to a constant factor by

$$\frac{i}{\hbar}[\mathbf{H}_0,\mathbf{K}] = 2\omega_0(2\mathbf{S}_{2,z} - \mathbf{S}_{2,x} - \mathbf{S}_{2,y}), \mathbf{S}_{2,j} = \sum_{i=1,A} (\mathbf{s}_{2,j})_i, \tag{14}$$

with

$$\mathbf{s}_{2,j} = \frac{i}{\hbar}[\mathbf{s}_{3,j},\mathbf{s}_{1,j}] = i[(\mathbf{b}^\dagger)_j^2 - \mathbf{b}_j^2]/4. \tag{15}$$

Therefore, Eq. (11) can be solved by a Slater determinant constructed using the eigenstates $|\psi\rangle(\lambda_k,\lambda_p)$ of the s.p. Hamiltonian

$$\mathbf{h}(\lambda_k,\lambda_p) = \mathbf{h}_0 - \lambda_k(2\mathbf{k}_z - \mathbf{k}_x - \mathbf{k}_y) - \lambda_p(2\mathbf{s}_{2,z} - \mathbf{s}_{2,x} - \mathbf{s}_{2,y}), \tag{16}$$

with $\lambda_k = c_0\lambda_q$ and $\lambda_p = 2\omega_0 c_0 \lambda_v$.

If $\lambda_p = 0$, then $\mathbf{h}(\lambda_k,0)$ is the Hamiltonian of a deformed harmonic oscillator with frequencies

$$\omega_x = \omega_y = \omega_0\sqrt{1+2\delta/3}, \quad \omega_z = \omega_0\sqrt{1-4\delta/3},$$

and $\delta = 3\lambda_k/2\hbar\omega_0$ the Nilsson deformation parameter. The eigenstates of $\mathbf{h}(\lambda_k,0)$ are related to those of $\mathbf{h}_0$ by unitary ''squeezing'' transformations $\mathbf{U}_\theta$ [23] and

$$\begin{aligned}\mathbf{h}(\lambda_k,0) &= \mathbf{h}_0 - 2\hbar\omega_0\delta\mathbf{K}/3 \\ &= \mathbf{U}_\theta\left[\sum_{j=x,y,z} \hbar\omega_j(\mathbf{b}_j^\dagger\mathbf{b}_j + 1/2)\right]\mathbf{U}_\theta^{-1},\end{aligned} \tag{17}$$

with

$$\mathbf{U}_\theta = e^{-i(\theta_x \mathbf{s}_{2,x} + \theta_y \mathbf{s}_{2,y} + \theta_z \mathbf{s}_{2,z})}, \quad \omega_j = \omega_0 e^{-\theta_j}. \tag{18}$$

When $\lambda_p \neq 0$, then

$$\mathbf{h}(\lambda_k,\lambda_p) = \mathbf{U}\mathbf{h}_{pq}\mathbf{U}^{-1}, \tag{19}$$

with

$$\mathbf{h}_{pq} = \sum_{j=x,y,z} E_j(\mathbf{b}_j^\dagger\mathbf{b}_j + 1/2)$$

and

$$\mathbf{U} = e^{ip(2\mathbf{k}_z - \mathbf{k}_x - \mathbf{k}_y)}\mathbf{U}_\theta, \quad E_j = \hbar\omega_0 e^{-\theta_j}. \tag{20}$$

Here $\theta_x = \theta_y = q$ and $\theta_z = -\ln\sqrt{3-6p^2-2e^{-2q}}$, such that

$$p = \frac{\lambda_p}{2\hbar\omega_0} \quad q = -\ln\sqrt{1+\frac{1}{\hbar\omega_0}\left(\lambda_k - \frac{\lambda_p^2}{4\hbar\omega_0}\right)}.$$

At $p=0$ the coordinate q is related to the Nilsson deformation parameter by $\delta = 3(e^{-2q}-1)/2$. The s.p. energy levels of the Nilsson model depend only on δ, but E_j represents a surface depending both on deformation and momentum parameters (q,p). Therefore, the Nilsson diagram of level crossings is the $p=0$ section in the more complex diagram of such intersecting energy surfaces.

The Hamiltonian $\mathbf{h}_{pq}$ is diagonal in the basis of the isotropic oscillator, and the two-parameter family of s.p. states $|\psi\rangle(\lambda_k,\lambda_p)$ may be generated by the unitary transformations $\mathbf{U}$ acting on the eigenstates $|r\rangle$ of $\mathbf{h}_0$. Thus, the solution

$|\Psi\rangle$ of Eq. (11) is given by the many-body correspondent $\mathcal{U}$ of $\mathbf{U}$ and the eigenstates $|r\rangle$.

The occupation number degree of freedom is included using the formalism of second quantization. In terms of the operators $c_\mu^\dagger$ creating fermions in the s.p. basis $|\mu\rangle$, $\mathbf{H}_0$ is

$$\mathbf{H}_0=\sum_{\mu,\nu}(\mathbf{h}_0)_{\mu\nu}c_\mu^\dagger c_\nu \tag{21}$$

and

$$\mathbf{H}_0-\lambda_k\mathbf{K}-\lambda_p(2\mathbf{S}_{2,z}-\mathbf{S}_{2,x}-\mathbf{S}_{2,y})=\mathcal{U}\left[\sum_{\mu,\nu}(\mathbf{h}_{pq})_{\mu\nu}c_\mu^\dagger c_\nu\right]\mathcal{U}^{-1}, \tag{22}$$

with

$$\mathcal{U}=e^{ip\mathbf{K}}e^{-i(\ln\sqrt{3-6p^2-2e^{-2q}}\mathbf{S}_{2,z}-q\mathbf{S}_{2,x}-q\mathbf{S}_{2,y})}. \tag{23}$$

If p and q are small, then

$$\mathcal{U}=e^{ip\mathbf{K}}e^{-iq(2\mathbf{S}_{2,z}-\mathbf{S}_{2,x}-\mathbf{S}_{2,y})}, \tag{24}$$

and up to constant factors is generated by the quadrupole coordinate and velocity operators. A similar unitary transformation generating both the phase and space shift of the s.p. orbitals was discussed in Ref. [24].

If the pairing interaction is included, then $\mathbf{H}_0$ in Eq. (11) should be replaced by $\mathbf{H}_0-G_{\rm pair}P^\dagger P/4$. Neglecting the terms containing commutators between the pairing and quadrupole operators, Eq. (11) becomes

$$\delta_\Psi\langle\Psi|\mathbf{H}_0-\frac{G_{\rm pair}}{4}P^\dagger P-\lambda_q\mathbf{Q}_0-\lambda_p\frac{i}{\hbar}[\mathbf{H}_0,\mathbf{Q}_0]|\Psi\rangle=0, \tag{25}$$

and making use of Eq. (22), it can be written as

$$\delta_\Psi\langle\Psi|\mathcal{U}\left[\sum_{\mu,\nu}(\mathbf{h}_{pq})_{\mu\nu}c_\mu^\dagger c_\nu\right]\mathcal{U}^{-1}-\frac{G_{\rm pair}}{4}P^\dagger P|\Psi\rangle=0. \tag{26}$$

Here

$$P^\dagger=\sum_{m=-j,j}(-1)^{j-m}c_{j,m}^\dagger c_{j,-m}^\dagger$$

denotes the pair creation operator and (j,m) are the angular momentum quantum numbers. In the arbitrary s.p. basis (μ), the pair creation operator will be written as $P^\dagger=\Sigma_\mu c_\mu^\dagger\bar{c}_\mu^\dagger$ the bar denoting time reversal. If $\mathcal{T}$ is the time reversal operator, this expression becomes

$$P^\dagger=\sum_{\mu,\nu}\langle\mu|\mathcal{T}\,|\nu\rangle c_\mu^\dagger c_\nu^\dagger.$$

Let us assume that in Eq. (26)

$$|\Psi\rangle=\mathcal{U}|\Psi_0\rangle, \tag{27}$$

with $|\Psi_0\rangle$ unknown. This function should be obtained from the variational equation

$$\delta_{\Psi_0}\langle\Psi_0|\sum_{\mu,\nu}(\mathbf{h}_{pq})_{\mu\nu}c_\mu^\dagger c_\nu-\frac{G_{\rm pair}}{4}P_U^\dagger P_U|\Psi_0\rangle=0, \tag{28}$$

where

$$P_U^\dagger=\mathcal{U}^{-1}P^\dagger\mathcal{U}=\sum_{\mu,\nu}\langle\mu|\mathbf{U}^{-1}\mathcal{T}\,\mathbf{U}|\nu\rangle c_\mu^\dagger c_\nu^\dagger. \tag{29}$$

In $\mathbf{U}$ the exponent $i\mathbf{s}_{2,k}$ is time reversal invariant, but $i(2\mathbf{k}_z-\mathbf{k}_x-\mathbf{k}_y)$ is not, and therefore

$$P_U^\dagger=\sum_{\mu,\nu}\langle\mu|e^{-2p(2\mathbf{k}_z-\mathbf{k}_x-\mathbf{k}_y)}|\nu\rangle c_\mu^\dagger\bar{c}_\nu^\dagger. \tag{30}$$

Equation (28) can be solved within the BCS or HFB approximations, depending on the choice of the basis (μ). If this basis is $|\mu\rangle=|r\rangle|s\rangle$, with $|r\rangle\equiv|n_x^r n_y^r n_z^r\rangle$ the eigenstates of $\mathbf{h}_0$ in Cartesian representation, and $|s\rangle$ the $j=1/2$ spinor, then the matrix $\langle\mu|h_{pq}|\nu\rangle$ is diagonal. Moreover, if the model space is restricted to a single oscillator shell containing M orbital states, and p is small, the matrix $\langle\mu|e^{-2p(2\mathbf{k}_z-\mathbf{k}_x-\mathbf{k}_y)}|\nu\rangle$ is also diagonal, and $|\Psi_0\rangle$ has the BCS form

$$|\Psi_0\rangle=e^{\Sigma_{r=1}^M(z_rP_r^\dagger-z_r^*P_r)}|0\rangle, \tag{31}$$

with $|0\rangle$ the particle vacuum,

$$P_r^\dagger=\Sigma_{m=\pm1/2}(-1)^{1/2-m}c_{r,m}^\dagger c_{r,-m}^\dagger,$$

and $z_r=\rho_re^{-i\phi_r}$ complex parameters. Therefore, the total trial wave function for the treatment of the quadrupole and pairing dynamics is

$$|\Psi\rangle=\mathcal{U}(p,q)e^{\Sigma_{r=1}^M(z_rP_r^\dagger-z_r^*P_r)}|0\rangle. \tag{32}$$

It depends on $2+2M$ parameters, the ''shape'' variables q,p, and the ''internal'' variables (ρ_r,ϕ_r), $r=1,M$.

The parameters ρ_r give the particle distribution on the levels of $\mathbf{h}_{pq}$ and when p,q are fixed Eq. (28) leads to the BCS equations. Their solution reflects the effect of the static ''Coriolis field'' $-\lambda_k\mathbf{K}-\lambda_p(2\mathbf{S}_{2z}-\mathbf{S}_{2x}-\mathbf{S}_{2y})$ on the structure of the ground state.

If the quadrupole moment and the shape variables are time dependent, we cannot assume that the changes in the structure are necessarily adiabatic. Therefore z_r should be considered independent variables and functions of time. The $(2+2M)$-dimensional manifold $\mathcal{M}$ of the trial states from Eq. (32), obtained considering p,q,z_r as independent variables, is embedded in the manifold $\mathcal{S}$ of the HFB states in the selected model space $[2M(2M-1)$ dimensional] and accounts for only the particular degrees of freedom of interest. The remaining $N_r=2M(M-1)-1$ degrees of freedom which are neglected will be included in the environment.

The classical phase-space structure on $\mathcal{M}$ is given by the matrix of the symplectic form $\omega^{\mathcal{M}}$ defined in Eq. (1). With respect to this structure the shape variables p,q considered above are not canonical, and

$$\omega_{pq}^{\mathcal{M}}=\hbar\{e^{q}(\langle\Psi_0|\mathbf{K}_x|\Psi_0\rangle+\langle\Psi_0|\mathbf{K}_y|\Psi_0\rangle)+\frac{4e^{-2q}}{(3-6p^2-2e^{-2q})^{3/2}}\langle\Psi_0|\mathbf{K}_z|\Psi_0\rangle\}. \quad (33)$$

For the internal dynamics it is convenient to use as variables the BCS phase angle ϕ_r and $p_r=(\sin2\rho_r)^2$, which equals half the expected number of particles in the orbital r [25]. These coordinates are canonical, such that

$$\omega_{p_r\phi_{r'}}^{\mathcal{M}}=-\hbar\,\delta_{rr'},\quad \omega_{p_rp_{r'}}^{\mathcal{M}}=0\quad \omega_{\phi_r\phi_{r'}}^{\mathcal{M}}=0. \quad (34)$$

All the other matrix elements of $\omega^{\mathcal{M}}$ which depend on both shape and internal variables contain the expected values of the commutators between pairing operators and $\mathbf{K}$ or $\mathbf{S}_{2,j}$ and will be neglected, to the same degree of approximation as assumed in Eq. (25).

Let us consider now Eq. (8) with $|\Psi\rangle$ given by Eq. (32) and

$$\mathbf{H}_0=\sum_{\mu,\nu}\langle\mu|\mathbf{h}_0|\nu\rangle c_\mu^\dagger c_\nu-\chi\mathbf{K}^2-\frac{G_{\rm pair}}{4}P^\dagger P, \quad (35)$$

the schematic Hamiltonian of the pairing plus quadrupole model [13]. With this choice Eq. (8) may be written in analytical form, and the numerical integration is simplified.

The average of the s.p. term in $\langle\Psi|\mathbf{H}_0|\Psi\rangle$ may be calculated using the following mean values:

$$\langle\Psi|\mathbf{S}_{3,j}|\Psi\rangle=\left(\cosh(q)+\frac{p^2}{2}e^{q}\right)\langle\Psi_0|\mathbf{S}_{3,j}|\Psi_0\rangle,\quad j=x,y, \quad (36)$$

$$\langle\Psi|\mathbf{S}_{3,z}|\Psi\rangle=\frac{2-p^2-e^{-2q}}{\sqrt{3-6p^2-2e^{-2q}}}\langle\Psi_0|\mathbf{S}_{3,z}|\Psi_0\rangle,$$

where $\langle\Psi_0|\mathbf{S}_{3,j}|\Psi_0\rangle=2\Sigma_r(\mathbf{S}_{3,j})_{rr}|v_r|^2=\Sigma_r(n_j^r+\frac{1}{2})|v_r|^2$, $v_r=e^{i\phi_r}\sin2\rho_r$, and $|v_r|^2=p_r$.

The average of the quadrupole-quadrupole interaction can be similarly calculated, and if the model space is a single oscillator shell,

$$\langle\Psi|\mathbf{K}^2|\Psi\rangle=\frac{1}{4}\left[\frac{4sk_z}{3-6p^2-2e^{-2q}}+e^{2q}(sk_x+sk_y)\right]+\langle\Psi|\mathbf{K}|\Psi\rangle^2, \quad (37)$$

with $sk_j\approx\Sigma_r|v_r|^2(n_j^r+1)$ and

$$\langle\Psi|\mathbf{K}|\Psi\rangle=\frac{2\langle\Psi_0|\mathbf{S}_{3,z}|\Psi_0\rangle}{\sqrt{3-6p^2-2e^{-2q}}}-e^{q}(\langle\Psi_0|\mathbf{S}_{3,x}|\Psi_0\rangle+\langle\Psi_0|\mathbf{S}_{3,y}|\Psi_0\rangle). \quad (38)$$

These terms are independent of ϕ_r and therefore they cannot change the occupation numbers p_r. Additional terms containing ϕ_r appear if more oscillator shells ($\Delta N=2$) are included.

The average of the pairing term $\langle\Psi|P^\dagger P|\Psi\rangle$ may be written as $\langle\Psi_0|P_U^\dagger P_U|\Psi_0\rangle=4|\Sigma_r M_r v_r u_r|^2$, $u_r=\sqrt{1-|v_r|^2}$, with $P_U^\dagger$ defined in Eq. (29) and

$$M_r=\langle r|e^{-2ip(f_x\mathbf{k}_x+f_y\mathbf{k}_y+f_z\mathbf{k}_z)}|r\rangle=M_x^rM_y^rM_z^r.$$

Here $f_x=f_y=-e^{q}$, $f_z=2e^{-\ln\sqrt{3-6p^2-2e^{-2q}}}$, and

$$M_j^r=\frac{1}{\sqrt{1+ipf_j}}\sum_{k=1}^{n_j^r}\frac{1}{4^{n_j^r-k}}\frac{n_j^r![2(n_j^r-k)]!}{(n_j^r-k)!^3k!}\left(-\frac{2ipf_j}{1+ipf_j}\right)^{n_j^r-k}. \quad (39)$$

In this expression p appears in the denominator, and decreases the pairing correlations when the shape is nonstationary.

With these results the Hamilton function on the right-hand side of Eq. (8) is

$$\mathcal{H}(p,q,p_r,\phi_r)\equiv\langle\Psi|\mathbf{H}_0|\Psi\rangle=\mathcal{H}_{\rm quad}(p,q,p_r)+\mathcal{H}_{\rm pair}(p,q,p_r,\phi_r), \quad (40)$$

where

$$\mathcal{H}_{\rm quad}(p,q,p_r)=2\hbar\omega_0\sum_r p_r\left\{\left(\cosh(q)+\frac{p^2}{2}e^{q}\right)\times(n_x^r+n_y^r+1)+\frac{2-p^2-e^{-2q}}{\sqrt{3-6p^2-2e^{-2q}}}\left(n_z^r+\frac{1}{2}\right)\right\}-\chi\langle\psi|\mathbf{K}^2|\psi\rangle$$

and

$$\mathcal{H}_{\rm pair}(p,q,p_r,\phi_r)=-G_{\rm pair}\left|\sum_r M_r^xM_r^yM_r^ze^{i\phi_r}\sqrt{p_r(1-p_r)}\right|^2.$$

Within the approximations implied above, $\mathcal{H}_{\rm pair}$ is the only term depending on the phase angles ϕ_r. In general, the total number of particles is an invariant of Eq. (8), but if $G_{\rm pair}=0$, then each occupation probability p_r becomes constant in time.

IV. NUMERICAL RESULTS

The formalism presented above can be applied to the isoscalar GQR of ^{28}Si observed in inelastic α particle [26] or electron [27] scattering experiments. The measured strength has the $E0$ and $E2$ components concentrated between 14 and 27 MeV. The centroids are located at $E_{\rm GMR}=17.9$ MeV and $E_{\rm GQR}=19.03$ MeV [26], corresponding to the excitation energies of the giant monopole and quadrupole resonances. The strength widths are $\Gamma_{\rm GMR}=4.8$ MeV and $\Gamma_{\rm GQR}=4.4$ MeV, respectively.

The ^{28}Si nucleus contains 12 particles outside the ^{16}O core, distributed over the 6 oscillator levels of the sd shell. This nucleus is one of the few light nuclei where collective behavior is observed, being attractive for microscopical studies. Its structure was investigated before using the SU(3) model [28], by the standard Hartree-Fock procedure [29], and in the generalized ''valley'' approximation [30]. In the Harvey model [21], the harmonic oscillator levels (n_x,n_y,n_z) of the sd shell which are occupied in the g.s. of

^{28}Si are (2,0,0), (1,1,0), and (0,2,0). Each level contains two protons and two neutrons, and the frequencies of the deformed oscillator potential are supposed to be in the ratio $\omega_z:\omega_x:\omega_y=2:1:1$. This ratio corresponds to $\delta=-0.75$, when a ''deformed shell'' structure occurs [31]. However, the total energy contour map shows that for ^{28}Si the g.s. minimum appears at a smaller deformation, $\delta\approx-0.45$.

If the ^{16}O core is assumed to be inert, the model space can be restricted to the six orbitals of the *sd* shell. According to the SU(3) classification, this model space carries the six-dimensional irreducible representation $(P,Q)=(2,0)$ [32], with (P,Q) the Cartan representation labels. The restriction to the valence particles reduces the volume of numerical calculations, but it should be taken with caution. For instance, the electrofission reaction $e+{}^{28}\mathrm{Si}\rightarrow e'+{}^{16}\mathrm{O}+{}^{12}\mathrm{C}$ is never produced with the both final nuclei in the ground state [21], indicating that during large amplitude motion of the valence nucleons, the core may get excited. Also, at deformations large as -0.75, the core level (0,0,1) becomes degenerate with the *sd* shell levels occupied by the valence particles.

The Hamiltonian of Eq. (40) will be considered further for a single kind of particles, protons, or neutrons. The ^{16}O core is accounted by adding 3 to $\langle\Psi_0|\mathbf{S}_{3,j}|\Psi_0\rangle$ in Eq. (36), representing the contribution of the inert levels. The residual interaction strengths are fixed here at $\chi=0.186$ MeV and $G_{\mathrm{pair}}=1.23$ MeV. For these values and six particles the present model has a metastable ground state (m.g.s.) at $\delta\approx-0.45$, with a quadrupole moment and pairing gap close to the values given by $\langle Q_0\rangle_{\mathrm{av}}=\sqrt{5/36\pi}A\langle r^2\rangle_0\delta=0.18\delta A^{5/3}$ fm^2 [33] and $\Delta_{\mathrm{av}}=12/\sqrt{A}$ MeV [13], respectively, when $A=28$.

Knowledge of the ground state is necessary first of all to fix the scale of the excitation energy. In the g.s. the energy has the absolute minimum, while the occupation probabilities p_r, $r=1,6$, and the shape variables (p,q) are constant in time. The g.s. parameters can be obtained by a time-independent search of the energy extremum, but the solution represents also the lowest energy critical point for the system of Eq. (2). This point can be found by the method of frictional cooling [34] consisting in solving Eq. (2) with random initial conditions and artificial dissipative terms on the right-hand side. If the trajectories are calculated for long enough time, the asymptotic state should be independent of the initial conditions, and very close to the true ground state.

This method shows that the Hamiltonian of Eq. (40) has no bounded minimum, because at large deformations the increase of the occupation numbers for the orbitals with large n_z makes the system unstable. This instability is related to the volume conservation condition [31], not considered here, and can be removed in a more refined treatment. However, in the physical region of oblate deformations there is a well-defined metastable ground state. This state occurs for the shape variables $p^g=0$, $q^g=0.137$ $[\beta_2=4\sqrt{\pi/5}(\delta/3)=4\sqrt{\pi/5}(e^{-2q}-1)/2=-0.43]$, and for the occupation probabilities p_r^g: $p^g_{(2,0,0)}=p^g_{(1,1,0)}=p^g_{(0,2,0)}=0.864$, $p^g_{(1,0,1)}=p^g_{(0,1,1)}=0.188$, and $p^g_{(0,0,2)}=0.032$. At this stationary point obtained by frictional cooling, the self-consistency equations for the quadrupole momentum and the pairing gap are fulfilled to a very good accuracy. Thus, the quadrupole moment is related to the deformation parameter by

$$\frac{\delta}{3}=\frac{\chi}{\hbar\omega_0}\langle\mathbf{K}\rangle, \tag{41}$$

and the BCS pairing gap $\Delta_g\equiv G_{\mathrm{pair}}\Sigma_{r=1}^{6}\sqrt{p_r^g(1-p_r^g)}=2.45$ MeV is the same as the one obtained from the self-consistent gap equations

$$\frac{2}{G_{\mathrm{pair}}}=\sum_{r=1}^{6}\frac{1}{\sqrt{\Delta^2+(E_r-\lambda)^2}}$$

$$N_{\mathrm{part}}=\sum_{i=1}^{6}\left[1-\frac{E_r-\lambda}{\sqrt{\Delta^2+(E_r-\lambda)^2}}\right], \tag{42}$$

with $N_{\mathrm{part}}=6$ and the s.p. energies E_r given by the partial derivatives

$$E_r=\frac{1}{2}\frac{\partial\mathcal{H}_{\mathrm{quad}}}{\partial p_r} \tag{43}$$

at the metastable point. One should note, however, that Δ_g is smaller than the gap extracted from the even-odd mass difference, $\Delta_{\mathrm{expt}}=4.4$ MeV [35].

If the system is not in the m.g.s., its evolution will be given by the set of 14 coupled TDHFB-Langevin equations

$$\sum_{j=1}^{14}\dot{x}^j\omega^{\mathcal{M}}_{jk}(\psi)=\frac{\partial\mathcal{H}}{\partial x^k}-\frac{\partial\langle\psi|\mathbf{K}|\psi\rangle}{\partial x^k}\times\left[\xi(t)-\gamma_K\frac{d\langle\psi|\mathbf{K}|\psi\rangle}{dt}\right]. \tag{44}$$

Here $x^{1,2}$ denotes the shape variables p,q and $\{x^j,j=3,8\}$ represents the six occupation probabilities p_r, while $\{x^j,j=9,14\}$ denotes the six BCS angles ϕ_r. The ''environment'' could be represented by the neglected degrees of freedom ($N_r=59$ when $M=6$), the core excitations, more complicated shape distortions, or particle emission channels. Because there is no detailed information about the strength of the coupling between this environment and the quadrupole dynamics, the coupling operator is chosen to be $\mathbf{K}$ and the spectrum of noise is assumed to be flat (white).

The symplectic form (Poisson bracket) $\omega^{\mathcal{M}}_{pq}$ depends on both shape and internal variables. Therefore, the classical phase-space structure of the shape dynamics changes in time, following the changes in the internal structure of the system.

Near the m.g.s., $\langle\mathbf{K}\rangle$ and ω_{pq} are well approximated by

$$\langle\mathbf{K}\rangle\approx-4.7+10.9\beta_2,\quad \omega^{\mathcal{M}}_{pq}\approx\hbar(33.4+13.6\beta_2), \tag{45}$$

and without environment coupling ($\gamma_K=0$) Eq. (44) shows the occurrence of small amplitude shape and pairing vibrations. The shape vibrations have two modes, one with high and the other with low frequency, $\Omega_s=19.6$ MeV/h, respectively $\Omega_p=1.9$ MeV/h ([18], p. 507). Ω_p is also the oscillation frequency of the occupation numbers p_r. Ω_s is very close to the random-phase-approximation (RPA) estimate $\sqrt{2}\omega_0/2\pi=19.1$ MeV/h [36], the small difference being produced essentially by pairing. However, the excitation energy in the small amplitude regime, when RPA is a valid approximation, is too small compared to E_{GQR}. Let us as-

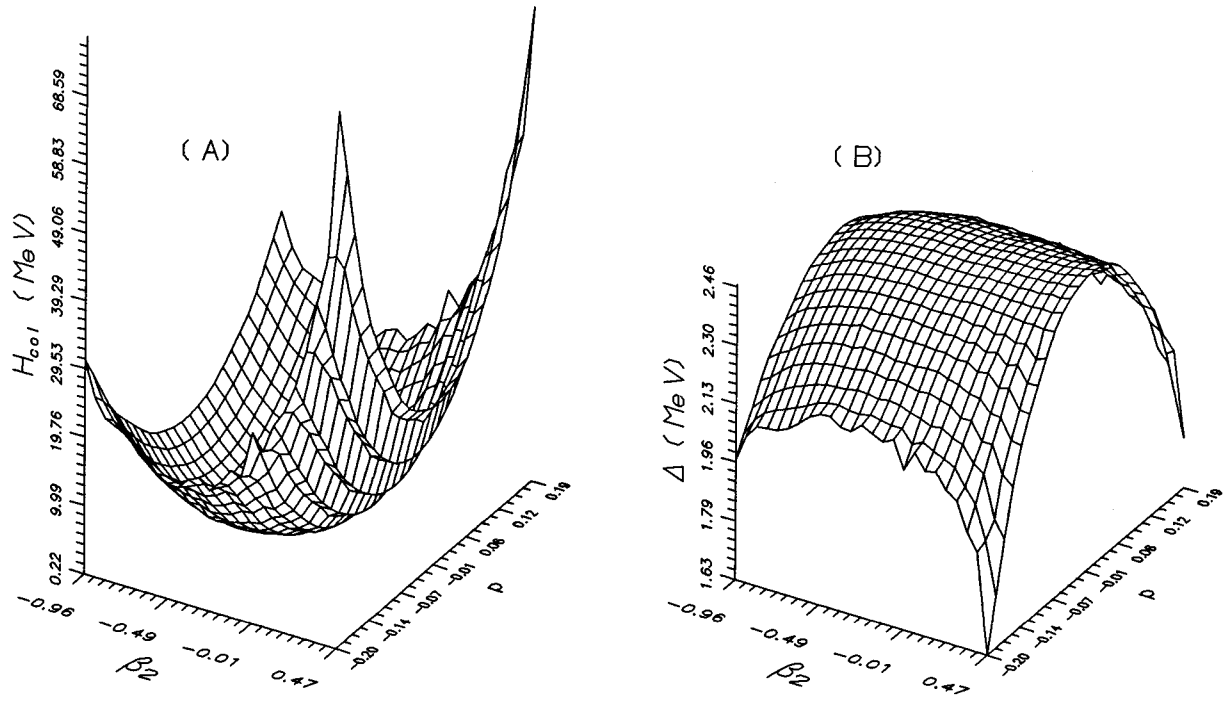

FIG. 1. Collective Hamiltonian (A) and pairing gap (B), calculated for the yrast configuration p_r^y, as a function of the quadrupole coordinate and momentum variables.

sume that the system increases its energy above the m.g.s. value by adiabatic deformation. If q and p are shifted from the metastable equilibrium point (p^g,q^g) in small steps ϵ_p,ϵ_q, then at each node of the lattice $(p^g+k_p\epsilon_p,q^g+k_q\epsilon_q)$, $k_{p,q}=\pm1,\pm2,\ldots$, the internal configuration (p_r,ϕ_r) can be determined from the condition of the minimum for the Hamiltonian $\mathcal{H}(p,q,p_r,\phi_r)$ in Eq. (40). This restricted minimization problem can be solved by frictional cooling of the intrinsic dynamics at each fixed couple of shape variables (p,q). The solution for this ''yrast'' internal configuration is represented by a set of 12 fields $p_r^y(p,q)$ and $\phi_r^y(p,q)$, $r=1,6$, over the shape phase space, and the total energy is given by a collective Hamilton function $H_{\rm col}(p,q)\equiv\mathcal{H}(p,q,p_r^y,\phi_r^y)$. In this calculation the lattice constants were fixed at $\epsilon_p=0.0133$ and $\epsilon_q=0.033$. The fields p_r^y and ϕ_r^y are almost constant, such that $p_r^y(p,q)\approx p_r^g$ and $\phi_r^y(p,q)\approx0$. The collective Hamilton function $H_{\rm col}$ is represented in Fig. 1(A). The pairing gap $\Delta=G_{\rm pair}|\Sigma_{r=1}^6 M_r v_r u_r|$ obtained for the yrast internal configuration is represented in Fig. 1(B). It depends weakly on q, but decreases strongly for large absolute values of the ''shape momentum'' p.

Without pairing, $H_{\rm col}$ reduces practically to $H_{\rm quad}^g(p,q)\equiv\mathcal{H}_{\rm quad}(p,q,p_r^g)$, and is represented for comparison in Fig. 2(A). The surface is almost the same as $H_{\rm col}(p,q)$ but shifted upwards by the m.g.s. pairing energy of 4.86 MeV. The symplectic form $\omega_{pq}^g\equiv\omega_{pq}^{\mathcal{M}}(p,q,p_r^g,\phi_r^g)$ is represented (in $\hbar$ units) in Fig. 2(B).

If $G_{\rm pair}=0$, the evolution takes place without changes in the internal structure along the closed orbits on the surface pictured in Fig. 2(A) which are fixed by the excitation energy. The trajectories can be found in this case by integrating the reduced system

$$\dot p\,\omega_{pq}^g=\frac{\partial H_{\rm quad}^g}{\partial q}\qquad \dot q\,\omega_{pq}^g=-\frac{\partial H_{\rm quad}^g}{\partial p}. \tag{46}$$

According to the requantization formalism [37], the closed orbits $\mathcal{O}_n$ selected by the integrality condition

$$\left|\int_{\Sigma_n} dpdq\,\omega_{pq}^g\right|=nh,\quad \mathcal{O}_n=\partial\Sigma_n,\quad n=1,2,3,\ldots, \tag{47}$$

are related to the eigenstates of the many-body system. For $n=1$ and small amplitudes this condition corresponds to the normalization of the RPA quasiboson operators [38]. In the present case it selects an orbit $\mathcal{C}$ with the excitation energy $E_{\mathcal{C}}=19.1$ MeV, very close to $E_{\rm GQR}$, and the oscillation frequency 15.5 MeV/h. This orbit was calculated choosing as initial conditions $p^0=0$, $q^0=0.65$ ($\delta=-1.1$), and has the ''phase-space'' representation shown in Fig. 3(A).

The closed orbit $\mathcal{C}$ is not a realistic correspondent of the GQR, because is stable, with infinite ''lifetime.'' In fact, the vibrational modes of the mean field are not isolated, but coupled with particle emission channels or compound nucleus configurations. Particle emission from low-lying excited states can be well described microscopically within the R-matrix formalism [39]. The GQR has relatively high energy, and the global effect of the interactions responsible for decay will be accounted for phenomenologically by the noise and friction terms in Eq. (44). With these terms, Eq. (46) changes into

$$\dot p\,\omega_{pq}^g=\frac{\partial H_{\rm quad}^g}{\partial q}-\frac{\partial\langle\mathbf{K}\rangle}{\partial q}\left[\xi(t)-\gamma_K\frac{d\langle\mathbf{K}\rangle}{dt}\right],$$

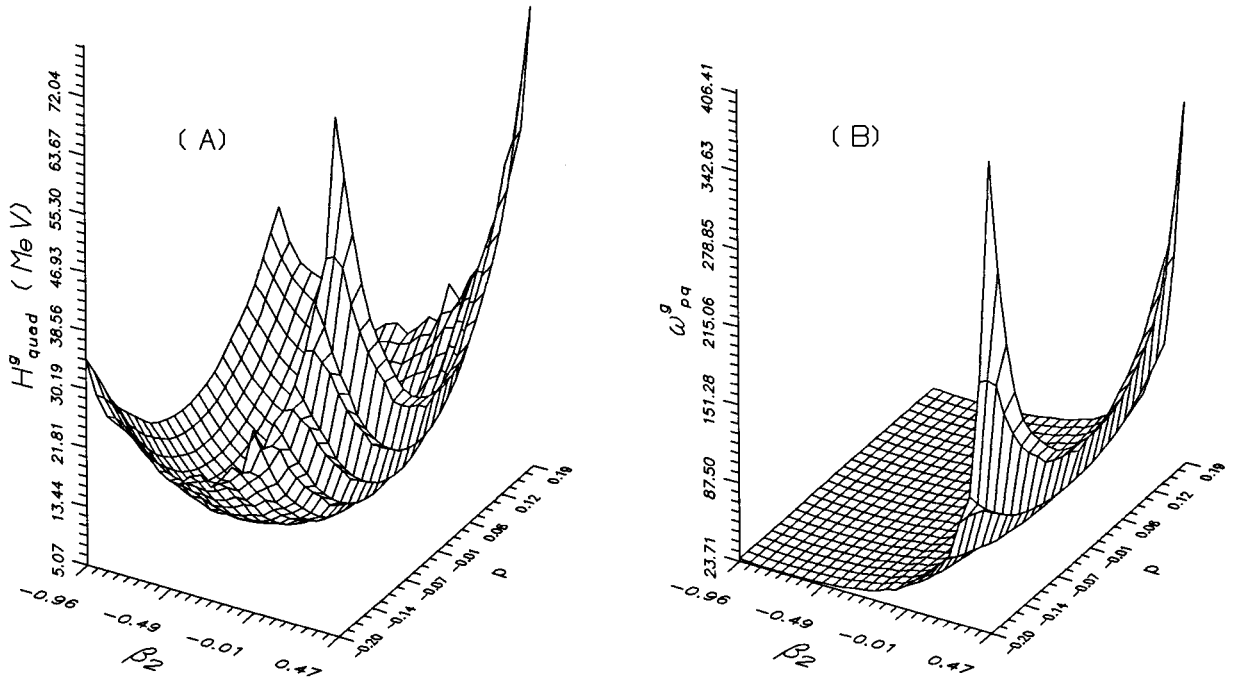

FIG. 2. Collective Hamiltonian (A) and symplectic form (in $\hbar$ units) (B), calculated at $G_{\text{pair}}=0$ for the ground state configuration p_r^g, as a function of the quadrupole coordinate and momentum variables.

$$\dot{q}\,\omega^g_{pq}=-\frac{\partial H^g_{\text{quad}}}{\partial p}+\frac{\partial\langle\mathbf{K}\rangle}{\partial p}\left[\xi(t)-\gamma_K\frac{d\langle\mathbf{K}\rangle}{dt}\right]. \tag{48}$$

The coefficient γ_K may be related to the friction constant γ_β in the β_2 coordinate simply equating the dissipation laws,

$$\gamma_K\left(\frac{d\langle\mathbf{K}\rangle}{dt}\right)^2=\gamma_\beta\left(\frac{d\beta_2}{dt}\right)^2. \tag{49}$$

Therefore, $\gamma_K=(d\langle\mathbf{K}\rangle/d\beta_2)^{-2}\gamma_\beta$, and using Eq. (45), one obtains $\gamma_K=\gamma_\beta/121$. Microscopic estimates of the diffusion coefficient $D_\beta=k_BT/\gamma_\beta$ in the *sd* shell are presented in Ref. [40]. In these calculations $T>0$, and γ_β is overestimated by a factor of 10, compared to the fission data.

The dissipation mechanism is beyond the purpose of the present work, but to fix a reference it is convenient to measure γ_β in terms of a virtual two-body viscosity coefficient μ, using the formula $\gamma_\beta=5R_0^3\mu=5(r_0)^3A\mu$ fm^3 [41]. Thus, for $A=28$, $\gamma_\beta/\hbar=229\mu$/TP (1 TP$=10^{11}$ N s/m^2 $=6.24\times10^{-22}$ MeV s/fm^3), and γ_K can be written as $\gamma_K/\hbar=1.9\mu$/TP.

If $T=0$ but $\gamma_K>0$, the noise vanishes and the excitation energy $E_x(t)$ decreases continuously, ressembling the decay process. The decay law of a quantum state changes in time, being quadratic for small times, exponential at intermediate times, and an inverse power at long times compared to the lifetime of the system [42]. The exponential stage is characterized by the decay width constant Γ, and in the present calculation this constant will be extracted from the excitation energy $E_x(t)$ by a one-parameter fit with the analytical function

$$E_I(t)=E_x(0)e^{-\Gamma_f t/\hbar}. \tag{50}$$

The dependence of the fit parameter Γ_f on μ is represented in Fig. 3(B). At weak friction the accuracy of the exponential fit is very good, and the system has damped oscillations with $\Gamma\approx1.53\times10^3\mu$ MeV/TP. Near $\mu\sim0.01$ TP, Γ_f attains a maximum and then decreases. At $\mu\sim0.022$ TP ($\Gamma_f=6.75$ MeV) the behavior changes from damped oscillations to aperiodic motion. The value Γ_{GQR} of ≈4.5 MeV can be therefore reproduced by two values of μ: one at weak friction, $\mu_1=0.002\,85$ TP, and the other in the aperiodic regime, $\mu_2=0.038$ TP. For these two cases $E_x(t)$ is represented by dashed line in Fig. 3(C) and Fig. 3(D), respectively.

It is interesting to note that in the aperiodic regime the fit provided by $E_{\text{I}}(t)$ is not very accurate, and $E_x(t)$ is closer to a quadratic function of time,

$$E_{\text{II}}(t)=E_x(0)e^{-\sigma^2t^2/\hbar^2}. \tag{51}$$

The dashed line in Fig. 3(D) is reproduced well by E_{II} with $\sigma=3.75$ MeV. A quadratic dependence similar to E_{II} was observed for the wave packets with a Gaussian strength distribution and the variance of the energy σ^2 [43].

At $T>0$ the thermal random forces lead to a Brownian diffusion of the shape variables. A typical orbit calculated with temperature and friction for the initial conditions of $\mathcal{C}$ is represented in Fig. 3(A). In this calculation $k_BT=2$ MeV, $\mu=0.038$ TP, and the time step of the numerical integration in Eq. (48) was $dt=0.0012\hbar$/MeV. At the moment $t_n=ndt$, the noise $\xi(t)$ was expressed by

$$\xi(t_n)=\sqrt{\frac{2k_BT\gamma_K}{dt}}R_n, \tag{52}$$

where R_n, $n=1,2,3,\ldots$ is a sequence of Gaussian random numbers with 0 mean and variance 1. This choice ensures

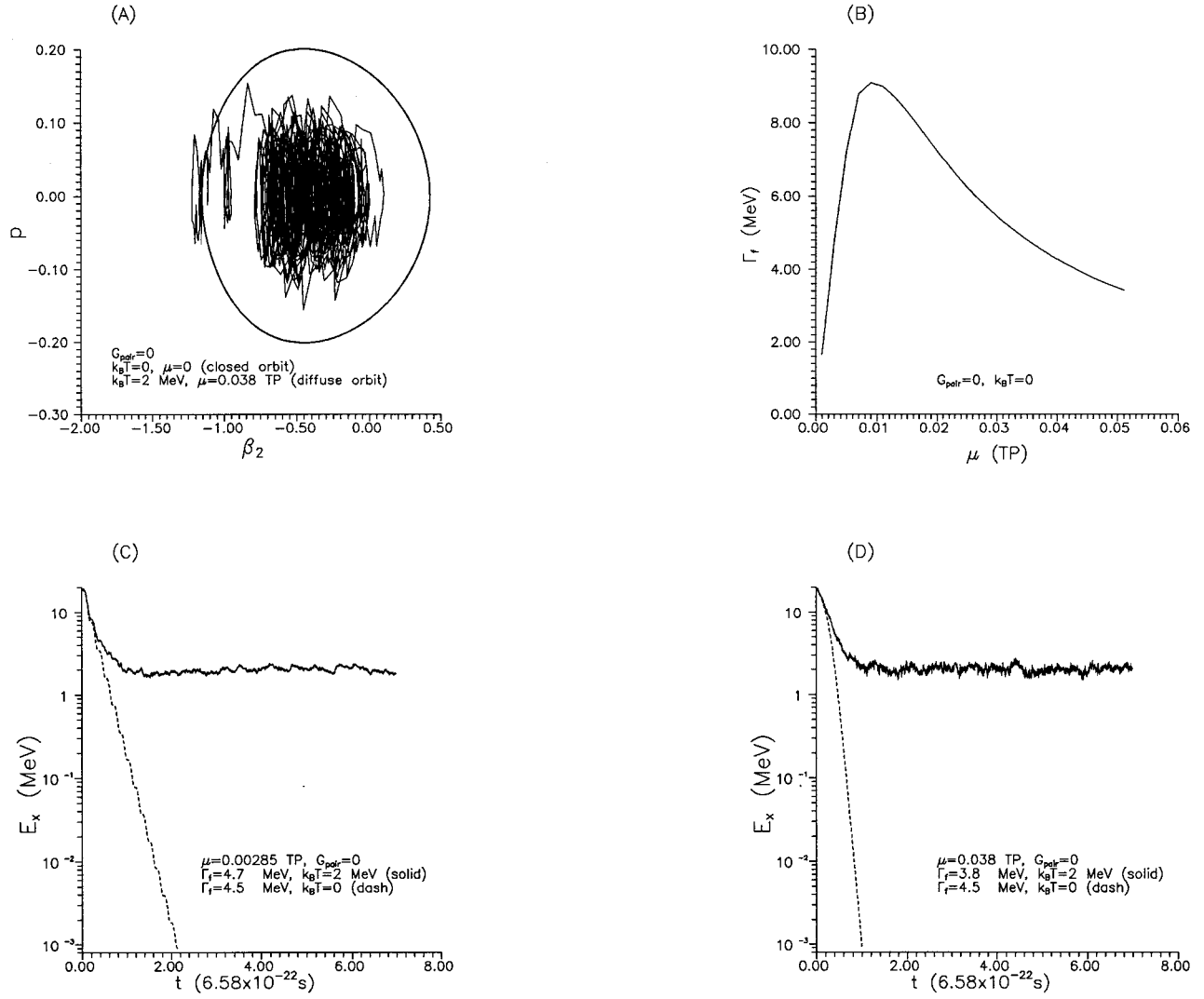

FIG. 3. Quadrupole shape dynamics without pairing. Phase-space orbits (A), decay constant as a function of the friction coefficient (B), $\langle\langle E_x\rangle\rangle_d$ (solid line) and E_x (dashed line) at $\mu=0.0028$ TP as a function of time (C), and $\langle\langle E_x\rangle\rangle_d$ (solid line) and E_x (dashed line) at $\mu=0.038$ TP as a function of time (D).

the discrete form of the fluctuation-dissipation theorem, $\langle\langle\xi(t_j)\xi(t_k)\rangle\rangle_d=2k_BT\gamma_K\delta_{t_jt_k}/dt$, with $\langle\langle\cdots\rangle\rangle_d$ denoting the average over an ensemble of trajectories.

With noise the excitation energy fluctuates instead of decreasing continuously, but the average over a long time interval is k_BT, proving that thermalization occurs. However, $E_x(t)$ along a single trajectory is not relevant for the calculus of the decay width, and instead it is necessary to use the average $\langle\langle E_x\rangle\rangle_d(t)$ of $E_x(t)$ over many trajectories, generated using different sequences of random numbers. The trial function for the fit in this case,

$$E_{\rm III}(t)=E_f+[E_x(0)-E_f]e^{-\Gamma_f t/\hbar}, \tag{53}$$

depends on two parameters Γ_f and E_f.

The average $\langle\langle E_x\rangle\rangle_d(t)$ was calculated over 100 trajectories at $k_BT=2$ MeV, for $\mu=0.002\,85$ TP [Fig. 3(C), solid line], and $\mu=0.038$ TP [Fig. 3(D), solid line]. The fit by $E_{\rm III}(t)$ gives in both cases E_f very close to 2 MeV, while Γ_f is 4.7 MeV and 3.8 MeV, respectively. These results are interesting, because they indicate that in the presence of the thermal environment Γ_f remains almost unchanged at weak friction, but decreases definitely in the overdamped regime.

The numerical results presented above were obtained neglecting the effects of the pairing interaction and keeping the occupation probabilities p_r fixed at the m.g.s. values. When the pairing interaction is switched on, instead of the reduced system of Eq. (48), in 2 variables, it is necessary to integrate the full system of Eq. (44), in 14 variables. The excitation energy $E_{\mathcal{C}}$ is obtained for the same initial conditions ($p=0$, $q=0.65$, $p_r=p_r^g$, $\phi_r=\phi_r^g$), and the corresponding orbit $\mathcal{C}_p$ of the shape variables, without friction at $T=0$, is pictured by the dashed line in Fig. 4(A). By contrast to $\mathcal{C}$, this trajectory is not closed, proving the existence of energy transfer between the pairing and shape degrees of freedom. The evolution of β_2 in the two cases, with and without pairing, is compared in Fig. 4(B). With pairing, the periodic quadrupole vibration acquires an amplitude and frequency modulation, but the effect is small. As in the case of a Toda lattice [44],

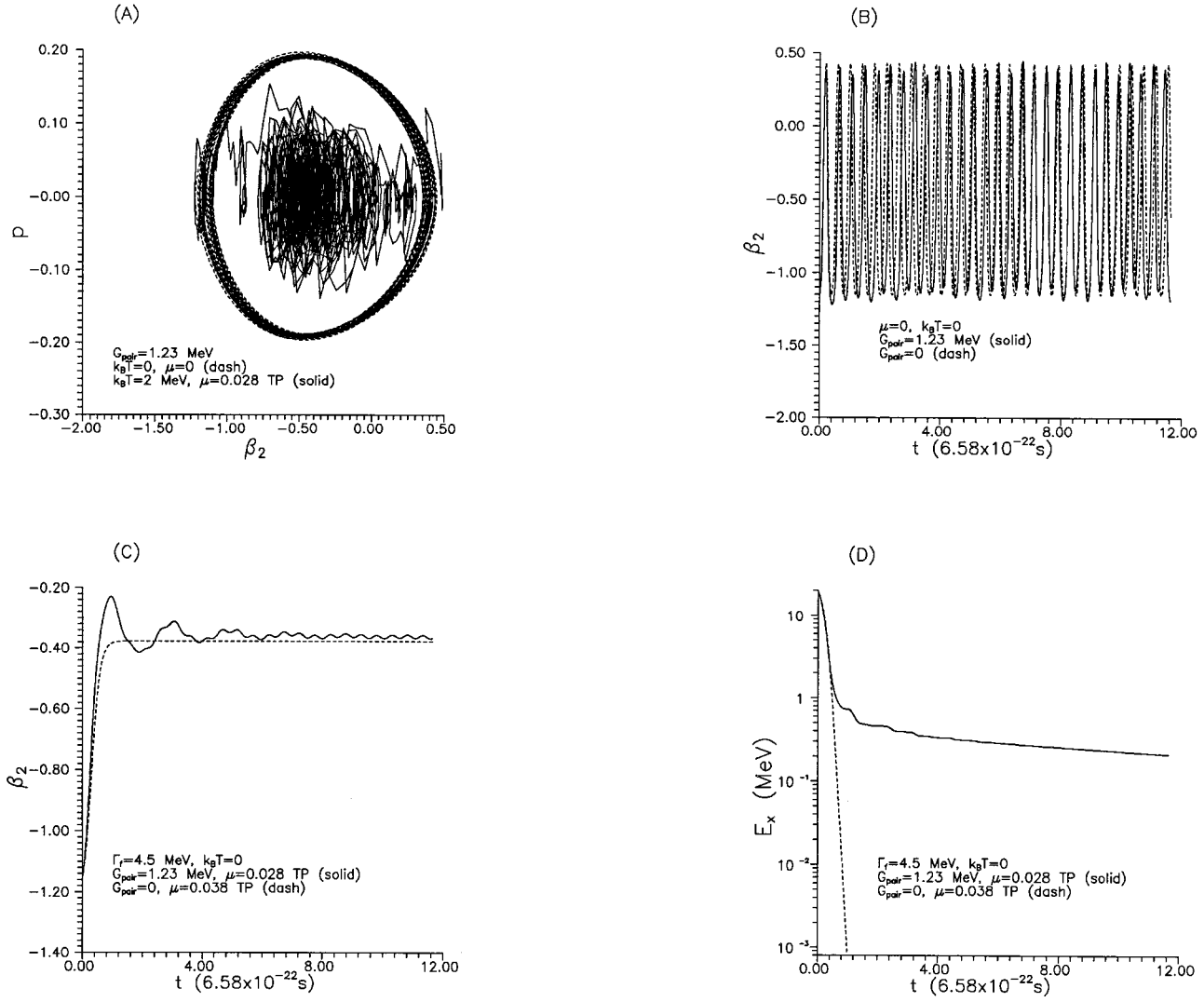

FIG. 4. Pairing effects on quadrupole shape dynamics. Phase-space orbits (A), β_2 as a function of time for $G_{\text{pair}}=1.23$ MeV (solid line) and $G_{\text{pair}}=0$ (dashed line) without environment coupling (B), β_2 as a function of time for $G_{\text{pair}}=1.23$ MeV (solid line) and $G_{\text{pair}}=0$ (dashed line) when $\Gamma_f=4.5$ MeV (C), and E_x as a function of time for $G_{\text{pair}}=1.23$ MeV (solid line) and $G_{\text{pair}}=0$ (dashed line) when $\Gamma_f=4.5$ MeV (D).

the relatively large number of variables and the highly nonlinear coupling do not produce necessarily a random behavior.

When $\gamma_K>0$, the integration of Eq. (44) with pairing shows a high sensitivity of the orbits with respect to the initial conditions. Thus, within a set of 100 trajectories starting at the same excitation energy from initial conditions chosen at random along $\mathcal{C}_p$, 92 are bounded and 8 are open. Along the bounded orbits the system evolves towards the m.g.s. ''adiabatically,'' dissipating energy without major changes of the occupation probabilities p_r. In the other case, before reaching the m.g.s., p_r has an irreversible evolution towards a prolate configuration p_r^* when $H^*_{\text{col}}(p,q) \equiv \mathcal{H}(p,q,p_r^*,\phi_r^*)$ has no finite minimum.

The adiabatic regime ressembles the case without pairing, though there is no clear transition from damped oscillations to aperiodic relaxation. Always there is a residual vibration of the shape and pairing variables with a frequency ~ 12.3 MeV/h, which is practically not affected by the friction force considered here. A similar situation was noticed in [9] where it was shown that the center of mass and squeezing degrees of freedom of the Gaussian wave packets require different dissipative terms. The decay constant Γ_f is calculated using the trial function $E_{\text{III}}(t)$. For the initial conditions of $\mathcal{C}$, the width Γ_f of 4.5 MeV is reproduced when $\mu=0.028$ TP. This value is smaller than μ_2, but very close to the one extracted from fission data, $\mu_{\text{expt}}=0.03\pm0.01$ TP [45]. The change produced by pairing on the adiabatic orbit having the initial excitation energy and the width Γ_f of the GQR is presented in Figs. 4(C) and 4(D). In general, for the adiabatic orbits calculated with pairing and friction Γ_f are below the curve of Fig. 3(B), and the residual energy does not exceed 1.5 MeV.

Along the unstable trajectories the shape variables have both an oscillatory and drift motion, while p_r evolves from the oblate configuration p_r^g to a prolate one, denoted generically by p_r^*. For instance, with the initial conditions of $\mathcal{C}$ and $\mu=0.002\,85$ TP the oblate-prolate inversion of population occurs at a time $\tau_{\text{inv}}\sim 0.5\hbar/\text{MeV}$, when the excitation energy

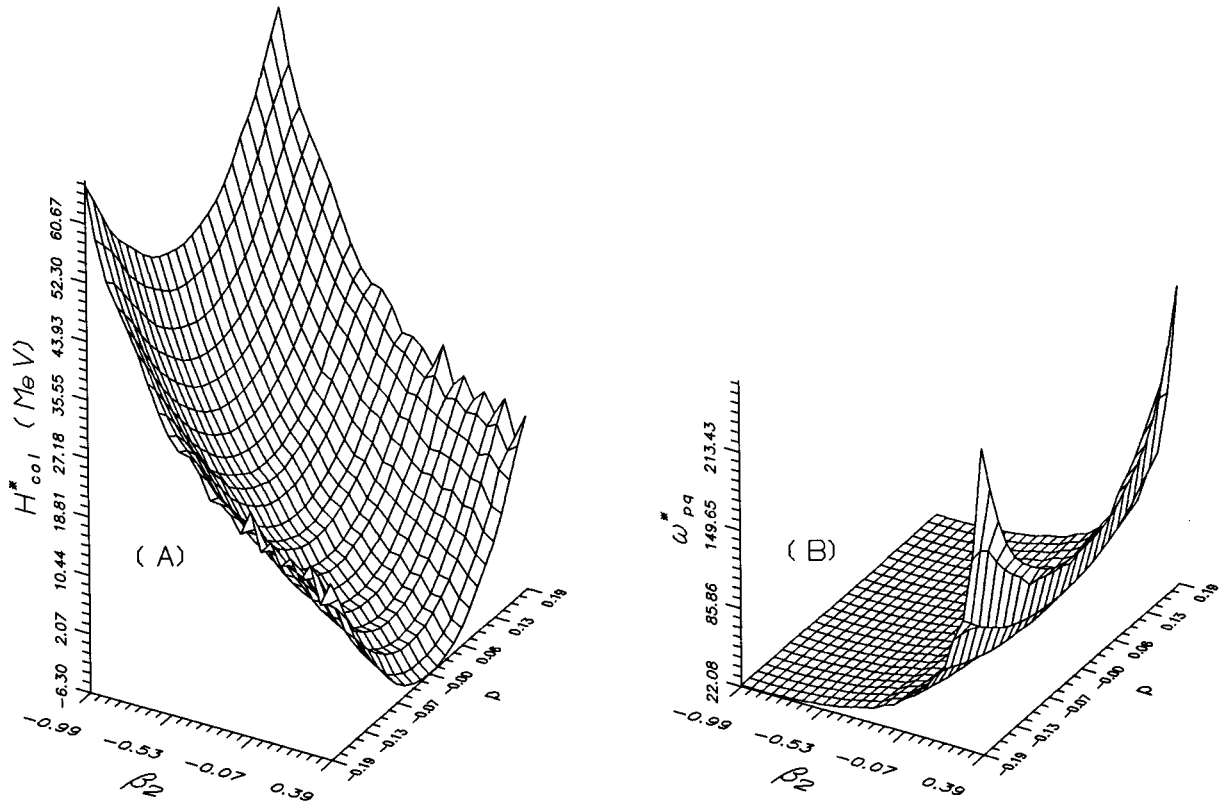

FIG. 5. Collective Hamiltonian (A) and symplectic form (in $\hbar$ units) (B), generated adiabatically for the prolate configuration p_r^*, as a function of the quadrupole deformation and momentum variables.

arrives below 5 MeV. At the transition time $\tau^* \sim 2\hbar/\mathrm{MeV}$, p_r becomes practically constant, $p^*_{(2,0,0)}=0.21$, $p^*_{(1,0,1)}=0.72$, $p^*_{(0,0,2)}=0.93$. After this moment the shape evolution is nonoscillatory, being produced by the new Hamiltonian structure $\{H^*_{\mathrm{col}}(p,q),\omega^*_{pq}\}$, pictured in Fig. 5.

The present study is completed by calculations for the case when pairing, friction, and temperature are all included. A typical orbit for the initial conditions of $\mathcal{C}$ with $k_BT=2$

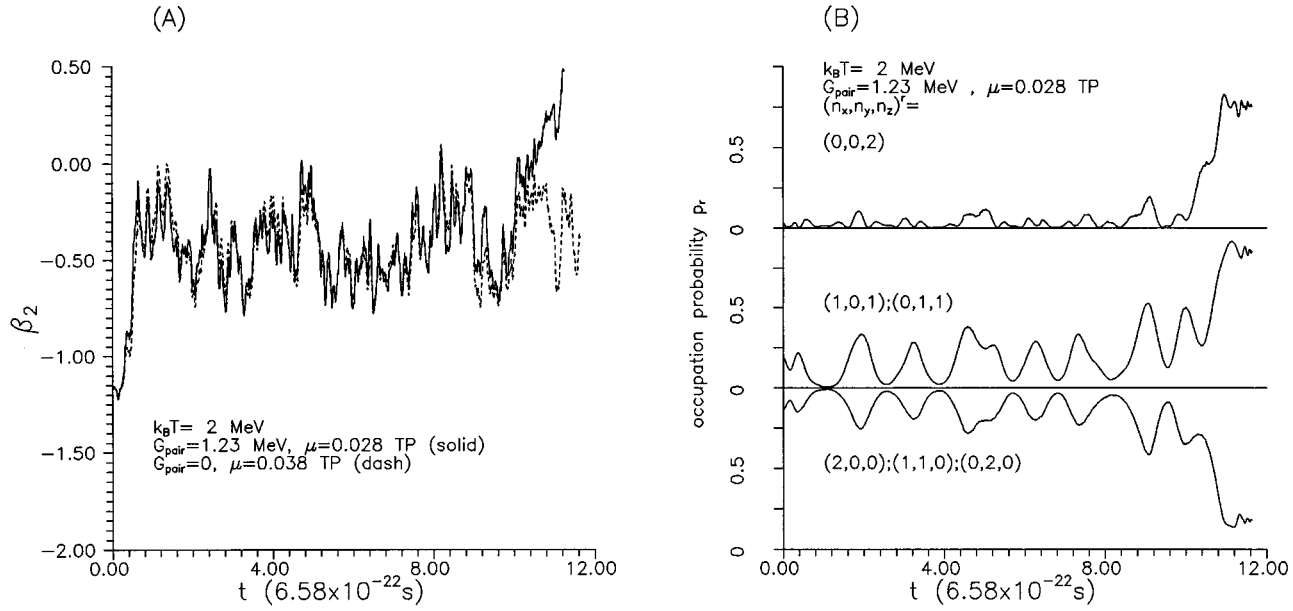

FIG. 6. Temperature effects on shape and internal dynamics. β_2 as a function of time for $G_{\mathrm{pair}}=1.23$ MeV (solid line) and $G_{\mathrm{pair}}=0$ (dashed line) (A), and occupation probabilities in the sd shell as a function of time (B).

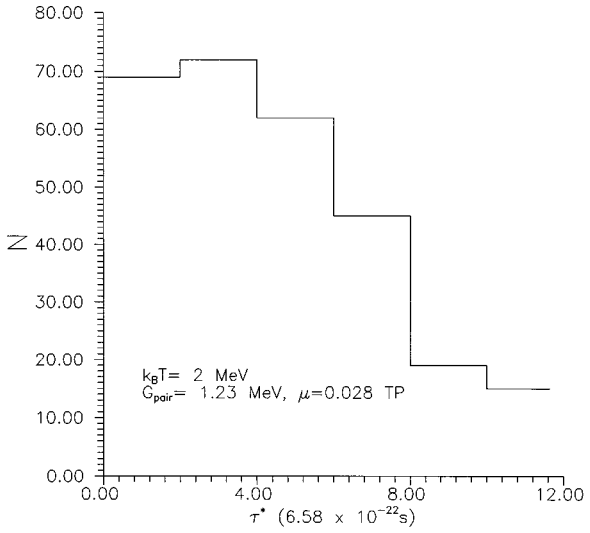

FIG. 7. Histogram of the configuration transition time τ^* for 300 trajectories calculated with $\mu=0.028$ TP and $k_BT=2$ MeV.

MeV and $\mu=0.028$ TP is represented in Fig. 4(A) by a solid line. The noise was chosen to be the same as in the calculation of the Brownian orbit shown in Fig. 3(A). The diffuse orbits of Figs. 3(A) and 4(A) are rather similar until $t\sim 10\hbar/$ MeV, but after this moment the orbit calculated with pairing escapes towards large prolate deformations, as can be seen from the trajectory plot of Fig. 6(A). This behavior is explained by the evolution of the occupation probabilities shown in Fig. 6(B), which change from p_r^g to a prolate configuration similar to p_r^*. The histogram of the transition time τ^* for 300 trajectories calculated with random initial conditions along $\mathcal{C}_p$ and $k_BT=2$ MeV is shown in Fig. 7.

V. SUMMARY AND CONCLUSIONS

In this work the problem of dissipative shape dynamics was treated within a TDHFB-Langevin formalism. The basic equations (7) were derived from the time-dependent variational principle, assuming a bilinear coupling between the quantum many-body system and a thermal environment (bath) composed of classical harmonic oscillators. In general, the coupling produces a memory friction term, but here we consider only the case of Ohmic dissipation [Eq. (8)]. This approach distinguishes between the friction (dissipation) and noise (temperature) effects on the many-body dynamics, and can be applied to the study of phenomena of decay, thermalization, or both.

For applications to the GQR dynamics, the manifold $\mathcal{S}$ of HFB trial functions is resticted to $\mathcal{M}$, of lower dimension, where only the quadrupole deformation and occupation number degrees of freedom are considered. The model space is also restricted to the sd shell, and numerical results are obtained for the case of ^{28}Si.

By construction, $\mathcal{M}$ is suited for the treatment of the quadrupole plus pairing Hamiltonian, and Eq. (8) related to this system was solved numerically for situations of increasing complexity: for the metastable g.s., small amplitude vibrations, and large amplitude GQR vibrations with or without pairing, friction, or temperature.

The ground state of ^{28}Si was generated by frictional cooling, and the test of self-consistency for the quadrupole and pairing mean fields was positive. The result is confirmed by the study of small amplitude quadrupole shape vibrations, which have the frequency expected for a self-consistent calculation.

Without pairing the internal configuration is fixed and the orbit of the shape variables is closed. Therefore, the system can be requantized by the Bohr-Wilson-Sommerfeld integrality condition of Eq. (47). The energy of the first excited state predicted by this method is very close to the GQR energy in ^{28}Si.

The decay constant was related to dissipation, and its dependence on the phenomenological friction coefficient is given in Fig. 3(B). At weak friction the decay is clearly exponential, as expected for a Breit-Wigner resonance, but at strong friction ressembles the decay of a state with a Gaussian strength distribution. This remark may be useful in the analysis of the experimental data.

At $T>0$ the shape variables have a Brownian trajectory (''shape diffusion'') and in the final stage of decay the motion is thermalized. The average over trajectories shows that before thermalization the decay law remains close to exponential, but the constant is different than at $T=0$. For $k_BT=2$ MeV thermalization occurs within $\sim 1\hbar/$MeV [Figs. 3(C) and 3(D)].

With pairing, the occupation probabilities may change in time adiabatically, namely, remaining near the oblate configuration of the metastable ground state, or they can have transitions to a prolate configuration. For an initial excitation energy of 19.1 MeV the evolution is definitely adiabatic if there is no dissipation [Fig. 4(B)]. With dissipation the evolution can be adiabatic or not, depending upon the magnitude of the friction coefficient and the initial conditions. The adiabatic dissipation carries the system close to the metastable ground state, but keeping a small residual excitation energy (stored in a pairing vibrational mode), which is weakly influenced by the present friction force [Fig. 4(D)]. For the nonadiabatic dissipative orbits, oblate $\rightarrow$ prolate configuration transitions occur relatively fast, within a time $\tau^* \sim 2\hbar/$MeV.

When $T>0$, the stage of adiabatic evolution is generally followed by the configuration transition, and consequently τ^* becomes spread over a wide interval (Fig. 7).

The results presented above indicate that transitions between different internal configurations during decay may be produced by dissipation alone, or by the combined effect of dissipation and noise. Extended investigations with temperature-dependent or memory friction may lead to realistic estimates of the shape diffusion coefficient.

ACKNOWLEDGMENTS

M.G. expresses his gratitude to Professor G. F. Bertsch for stimulating discussions on the initial aspects of this work, to Professor P. Schuck for constructive remarks on the present approach to the many-fermion dynamics, and to Professor V. Zelevinsky for valuable comments on the self-consistency problem.

[1] S. E. Koonin and J. Randrup, Nucl. Phys. **A289**, 475 (1977).
[2] J. Blocki, Y. Boneh, J. R. Nix, J. Randrup, M. Robel, A. J. Sierk, and W. J. Swiatecki, Ann. Phys. (N.Y.) **113**, 330 (1978).
[3] J. R. Nix, D. G. Madland, and A. J. Sierk, in *Nuclear Data for Basic and Applied Science*, Vol. 1, Proceedings of the International Conference, Santa Fe, New Mexico, May 1985, edited by P. G. Young, R. E. Brown, G. F. Auchampaugh, P. W. Lisowski, and L. Stewart, LANL, p. 263.
[4] N. Carjan, A. J. Sierk, and J. R. Nix, Nucl. Phys. **A452**, 381 (1986).
[5] T. Wada, Y. Abe, and N. Carjan, Phys. Rev. Lett. **70**, 3538 (1993).
[6] W. Bauer, D. McGrew, V. Zelevinsky, and P. Schuck, Phys. Rev. Lett. **72**, 3771 (1994).
[7] F. Barranco, R. A. Broglia, and G. F. Bertsch, Phys. Rev. Lett. **60**, 507 (1988).
[8] U. Mosel, P.-G. Zint, and K. H. Passler, Nucl. Phys. **A236**, 252 (1974).
[9] M. Grigorescu and N. Carjan, Phys. Rev. E **51**, 1996 (1995).
[10] H. A. Weidenmüller, Nucl. Phys. **A502**, 387c (1989).
[11] N. Auerbach and A. Yeverechyahu, Ann. Phys. (N.Y.) **95**, 35 (1975).
[12] F. E. Bertrand, Nucl. Phys. **A354**, 129c (1981).
[13] P. Ring and P. Schuck, *The Nuclear Many-Body Problem* (Springer, New York, 1980).
[14] P. Kramer and M. Saraceno, *Geometry of the Time-Dependent Variational Principle in Quantum Mechanics*, Lecture Notes in Physics Vol. 140 (Springer, New York, 1981).
[15] M. Grigorescu, in *Collective Motion and Nuclear Dynamics*, edited by A. A. Raduta, D. S. Delion, and I. I. Ursu (World Scientific, Singapore, 1996), p. 251.
[16] P. Hänggi, P. Talkner, and M. Borkovec, Rev. Mod. Phys. **62**, 251 (1990).
[17] M. Grigorescu and N. Carjan, Rom. J. Phys. **41**, 53 (1996).
[18] A. Bohr and B. R. Mottelson, *Nuclear Structure* (W. A. Benjamin, New York, 1975), Vol. II.
[19] S. Raman *et al.*, At. Data Nucl. Data Tables **36**, 2 (1987).
[20] M. Grigorescu, in *Frontier Topics in Nuclear Physics*, edited by W. Scheid and A. Sandulescu (Plenum Press, New York, 1994), p. 491.
[21] B. R. Fulton and W. D. M. Rae, J. Phys. G **16**, 333 (1990).
[22] M. Harvey, in Proceedings of the 2nd Conference on Clustering Phenomena in Nuclei, 1975, College Park, 1975 USDERA Report No. ORO-4856-26 (unpublished), p. 549.
[23] M. Grigorescu, Institute of Atomic Physics, Bucharest, Report No. FT-326-1988, 1988.
[24] G. F. Bertsch, *Frontier and Borderlines in Many-Particle Physics* (CIV, Corso, Italy, 1988), p. 41.
[25] A. A. Raduta, V. Ceausescu, A. Gheorghe, and M. Popa, Nucl. Phys. **A427**, 1 (1984).
[26] Y.-W. Lui *et al.*, Phys. Rev. C **31**, 1643 (1985).
[27] Th. Kihm *et al.*, Phys. Rev. Lett. **56**, 2789 (1986).
[28] J. P. Bernier and M. Harvey, Nucl. Phys. **A94**, 593 (1967).
[29] S. Das Gupta and M. Harvey, Nucl. Phys. **A94**, 602 (1967).
[30] N. R. Walet, G. Do Dang, and A. Klein, Phys. Rev. C **43**, 2254 (1991).
[31] I. Ragnarsson, S. G. Nilsson, and R. K. Sheline, Phys. Rep. **45**, 1 (1978).
[32] M. Grigorescu, St. Cerc. Fiz. **36**, 3 (1984).
[33] T. Suzuki and D. J. Rowe, Nucl. Phys. **A289**, 461 (1977).
[34] H. Horiuchi, Nucl. Phys. **A522**, 257c (1991).
[35] P. U. Sauer, A. Faessler, H. H. Wolter, and M. M. Stingl, Nucl. Phys. **A125**, 257 (1969).
[36] D. R. Bes, R. A. Broglia, and B. S. Nilsson, Phys. Rep. **16**, 1 (1975).
[37] K.-K. Kan, J. J. Griffin, P. C. Lichtner, and M. Dworzecka, Nucl. Phys. **A232**, 109 (1979).
[38] M. Grigorescu, Rom. J. Phys. **38**, 859 (1993).
[39] M. Grigorescu, B. A. Brown, and O. Dumitrescu, Phys. Rev. C **47**, 2666 (1993).
[40] B. W. Bush, G. F. Bertsch, and B. A. Brown, Phys. Rev. C **45**, 1709 (1992).
[41] J. R. Nix and A. J. Sierk, Phys. Rev. C **21**, 396 (1980).
[42] A. Peres, Ann. Phys. (N.Y.) **129**, 33 (1980).
[43] M. Grigorescu and N. Carjan, Report No. CNRS-IN2P3-CENBG-9507, 1995.
[44] M. Toda, Phys. Rep. C **18**, 1 (1975).
[45] K. T. R. Davies, R. A. Managan, J. R. Nix, and A. J. Sierk, Phys. Rev. C **16**, 1890 (1977).